Supplementary Information

Probing the Nucleobase-Specific Binding Interaction of Hydroxychloroquine Sulfate with RNA and Subsequent Sequestration by a Water-Soluble Molecular Basket

Rahul Yadav, Subhasis Das, Madhumita Mukherjee and Saptarshi Mukherjee*

Department of Chemistry,

Indian Institute of Science Education and Research Bhopal, Bhopal Bypass Road,

Bhopal 462 066, Madhya Pradesh, India

**Corresponding author: E-mail: saptarshi@iiserb.ac.in, orcid.org/0000-0001-8280-0754*

1. Experimental Section:

1.1 Materials. Torula yeast RNA^{Phe} (RNA), Hydroxychloroquine Sulphate (HCQS), Adenosine 5'-monophosphate disodium salt (AMP), Guanosine 5'-monophosphate (GMP) disodium salt hydrate, Cytidine 5'-monophosphate (CMP), Uridine 5'-monophosphate (UMP), ethidium bromide (EtBr), Hoechst 33258, calf thymus DNA (ct-DNA), polyadenylic acid-polyuridylic acid sodium salt, homopolymer RNA duplex (Poly(A).Poly(U)), potassium ferrocyanide, 4-Sulfocalix[4]arene (SCX4), sodium chloride, monosodium phosphate and disodium phosphate were procured from Sigma-Aldrich and used at received. 20 mM phosphate buffer of pH ~ 7.4 was prepared with monosodium phosphate and disodium phosphate and it was used for all the spectroscopic and calorimetric experiments. The stock solution of RNA and nucleotides was prepared in a buffer. The concentration of RNA was determined spectrophotometrically using molar absorption coefficient A_{258} = 10405 M^{-1} cm^{-1}.[S1] The purity of the RNA solution was also verified spectrophotometrically by monitoring the A_{260}/A_{280} ratio, which was found to be 2.1 (for pure the A_{260}/A_{280} ~ 2.0).[S2] Solutions of Potassium Ferrocyanide, NaCl, HCQS, Hoechst, EtBr, and SCX4 were prepared in Milli-Q water. All the measurements were performed at 298 K unless a specific temperature is mentioned.

A single monomeric unit of torula yeast RNA consists of 76 nucleobases, making the cloverleaf-like secondary structure. According to 6TNA PDB (available on the RSCB website), a collective proportion of each RNA nucleobase (unmodified and modified nucleobases) is tabulated in Table S1.

Table S1 Percentage proportion of nucleobases present in torula yeast RNA.

S.N.	Nucleobase (one letter code)	Number of unmodified nucleobases	Number of modified nucleobases	Number of total nucleobases	% proportion of each nucleobase
1.	G	18	5	23	30.26%
2.	A	17	1	18	23.68%
3.	U	13	5	18	23.68%
4.	C	15	2	17	22.37%
	Total	**63**	**13**	**76**	**99.99%**

1.2 Methods.

A. Steady-state Absorption and Fluorescence Spectroscopy: Steady-state absorption spectra were acquired in a Cary 100 UV-Vis spectrophotometer with proper baseline correction. Steady-state fluorescence emission spectra were recorded in Fluorolog 3-111 spectrofluorometer. A quartz cuvette of 1 cm path length was used for all the spectroscopic measurements. The fluorescence spectra for HCQS samples were recorded at excitation wavelengths of 330 nm with 2 and 3 nm excitation and emission slit widths, respectively. Ethidium bromide samples were excited at 480 nm and Hoechst samples were excited at 350 nm. Apparent binding constants for RNA-HCQS binding interactions were estimated from the Benesi-Hildebrand equation using the modulations in fluorescence and absorbance spectral profiles, independently.

$$\frac{1}{\Delta F} = \frac{1}{\Delta F_{max}} + \frac{1}{K_B(\Delta F_{max})} \times \frac{1}{[RNA]} \qquad (1)$$

Here, ΔF = (Fluorescence intensity of free HCQS – RNA bound HCQS), ΔF_{max} = difference in the fluorescence intensity at the highest RNA concentration. The apparent binding constant (K_B) is determined from the intercept-to-slope ratio of the linear plot.

The same equation was also applied to analyze the absorption data as outlined below.

$$\frac{1}{\Delta A} = \frac{1}{\Delta A_{max}} + \frac{1}{K_B(\Delta A_{max})} \times \frac{1}{[RNA]} \qquad (2)$$

Here, ΔA = (Absorbance of free HCQS – Absorbance of RNA bound HCQS), ΔA_{max} = maximum difference in the absorbance of free HCQS and RNA bound HCQS. The apparent binding constant (K_B) is determined from the intercept-to-slope ratio of the linear plot.

B. Fluorescence Lifetime Measurements: Fluorescence lifetime measurements for HCQS samples, in the absence and presence of RNA, were recorded using an IBH Nano LED, source N-340, a picosecond diode laser. The Instrument Response Function (IRF) of the laser source was recorded by using LUDOX as a scatterer, and the value was obtained to be ~ 750 ps. The lifetime decay functions were fitted using a multi-exponential equation:[S3]

$$I(t) = \sum A_i e^{-\frac{t}{\tau_i}} \qquad (3)$$

where, A_i is the pre-exponential factor of i^{th} lifetime component(τ_i). χ^2 indicates the goodness of fitting. The average lifetime $<\tau>$ of the samples was calculated using the equation given below:[S3]

$$<\tau> = \frac{\sum \tau_i \alpha_i}{\sum \alpha_i} \quad (4)$$

where, α_i is the relative amplitude of the i^{th} lifetime component(τ_i).

C. Circular Dichroism Spectroscopy: Circular dichroism (CD) spectral measurements for RNA samples were recorded in a JASCO J-815 spectropolarimeter using a 1 mm path-length quartz cuvette. All the spectra were recorded with proper baseline correction. The final CD spectrum is an average of two accumulations with a scan rate of 100 nm min^{-1}. The CD spectra were collected in a wavelength range of 200 to 390 nm for both, the addition of HCQS in RNA solution and *vice-versa* to acquire induced circular dichroism (ICD) spectra.

D. Isothermal Titration Calorimetric Studies: Isothermal titration calorimetry (ITC) experiments were performed with a MicroCal PEAQ-ITC instrument (Malvern Instruments). Titrations were performed keeping a reference power of 10 µcal s^{-1} and a delay between the injections of 150 s. The first injection volume (0.4 µL) was rejected before data analysis. Subsequent titration steps involved 19 injections with 2 µL each. The syringe contained the RNA solution ([RNA] = 10 mM) and the cell contained the HCQS ([HCQS] = 200 µM) solution in the buffer. Heat of dilution was determined by titrating free RNA into a buffer under identical experimental conditions. For temperature-dependent experiments, a range of temperatures from 293 K to 313 K was varied keeping all the parameters the same. A similar procedure was followed for monitoring the interaction of HCQS with the nucleobases where [nucleobase] = 10 mM in the cell, and [HCQS] = 1 mM in the syringe for AMP, GMP, and CMP nucleobases and [HCQS] = 1.5 mM for UMP nucleobase). Additionally, for the sequestration experiments, 100 µM HCQS was kept in the cell and 1 mM SCX4 was kept in the syringe for binding interactions of SCX4 with HCQS (in the absence of RNA) and 100 µM HCQ with 10 mM RNA, was kept in the cell and 1 mM SCX4 was kept in the syringe for binding interactions of SCX4 with RNA-bound HCQS. Control experiments corresponding to these were carried out by titrating only 1 mM SCX4 in blank buffer and only 10 mM RNA (without HCQS). Final corrected heat change data was fitted in MicroCal PEAQ-ITC Analysis

Software with a single set of sites binding model and corresponding thermodynamic parameters were obtained.[S4]

E. Molecular Docking Studies: The molecular docking studies were performed in Autodock 4.2 software. PDB IDs for RNA (6TNA) and for 4-sulfocalix[4]arene (6HA4) were downloaded from the RCSB protein data bank. The structure of Hydroxychloroquine was optimized in the Gaussian 09 package. The parameters used for docking are as follows: grid map dimensions (126, 126, 126) for (x,y,z) axes, grid point spacing was for RNA (0.719 Å) and for SCX4 (0.375 Å). Genetic Algorithm (GA) parameters: population size was 150, GA maximum energy evaluation was 250,000, and 100 runs were kept for both. Postdocking analysis and three-dimensional visualizations were conducted using UCSF Chimera 1.17.3 software.[S5]

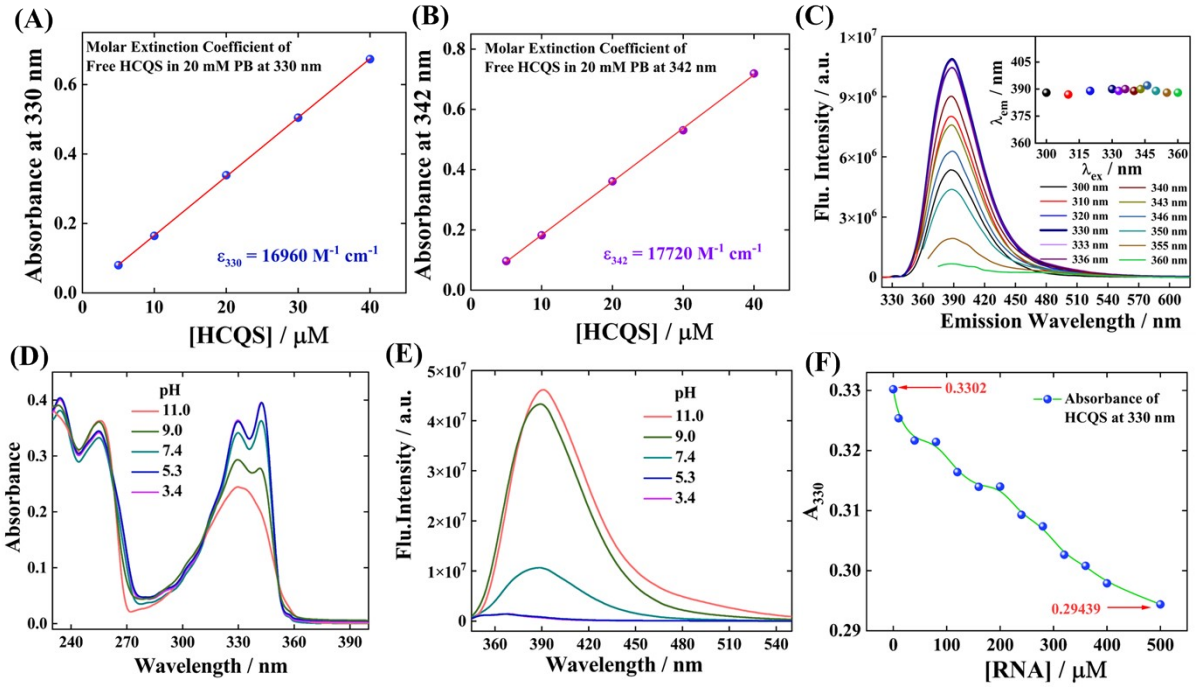

Fig. S1 Molar extinction coefficient of HCQS at (A) 330 nm and, (B) 342 nm in 20 mM PB. (C) Excitation-dependent emission spectra of HCQS. The inset represents the non-variant nature of emission maxima at different excitation wavelengths. (D) Absorption spectra of HCQS at different pH. (E) Emission spectra of HCQS at different pH. (F) Variations in the absorbance of HCQS (monitored at 330 nm) with the incremental addition of RNA.

1.3 Estimation of fraction of free HCQS and RNA-bound HCQS.

Approach I: In our present investigation, we have used an initial concentration of HCQS of 20 μM, to which we added RNA up to a concentration of 500 μM. To estimate the fraction of bound HCQS to RNA, we used the following binding equilibrium:

$$RNA + HCQS \rightleftharpoons RNA{:}HCQS$$

The association constant, $K_a = \frac{[RNA{:}HCQS]}{[RNA][HCQS]}$, and the dissociation constant was determined by $K_d = 1/K_a$.

Thus, dissociation constant $K_d = \frac{[RNA][HCQS]}{[RNA{:}HCQS]}$

Here, [RNA], [HCQS], [RNA:HCQS] are the concentrations of RNA, HCQS, RNA:HCQS respectively, at equilibrium. So, [RNA:HCQS] was the final concentration of bound RNA as well as the bound HCQS. Hence, the concentration of HCQS at equilibrium, [HCQS] = $[HCQS]_0$ – [RNA:HCQS], where $[HCQS]_0$ = the initial concentration of HCQS (=20 μM). As [RNA] is much greater than [HCQS], we can say that initial [RNA], i.e. $[RNA]_0 \approx [RNA]$ = 500 μM).

So, K_d now can be re-written as:

$$K_d = \frac{[RNA]_0\,([HCQS]_0 - [RNA{:}HCQS])}{[RNA{:}HCQS]}$$

By rearranging,

$$K_d[RNA{:}HCQS] = [RNA]_0\,([HCQS]_0 - [RNA{:}HCQS]_)$$

$$K_d[RNA{:}HCQS] = [RNA]_0\,[HCQS]_0 - [RNA]_0\,[RNA{:}HCQS]$$

$$K_d[RNA{:}HCQS] + [RNA]_0\,[RNA{:}HCQS] = [RNA]_0\,[HCQS]_0$$

$$\frac{[RNA{:}HCQS]}{[HCQS]_0} = \frac{[RNA]_0}{K_d + [RNA]_0} \qquad (5)$$

This equation represents the fraction of HCQS that is bound to RNA.

From the absorption data, K_a has been estimated to be 1.56×10^3 M^{-1} (corresponding to a K_d value of 641 μM), and $[RNA]_0$ = 500 μM, then with respect to the initial concentration of HCQS (which is constant at 20 μM), the bound fraction of HCQS (using equation 5) will be 0.44, and the fraction of free HCQS will be 0.56.

Approach II: As an alternative approach, we also estimated the concentration of free HCQS and RNA-bound HCQS using the modified Benesi-Hildebrand equation.

The abovementioned version of the Benesi-Hildebrand equation (equation 2) can also be rewritten in terms of the molar extinction coefficient (at a particular wavelength) of free and bound chromophores.[S6,S7]

$$\frac{1}{\Delta A} = \frac{1}{(\varepsilon_f - \varepsilon_b)L_T} + \frac{1}{K_B\,(\varepsilon_f - \varepsilon_b)L_T} \times \frac{1}{[RNA]} \qquad (6)$$

Here, ε_f and ε_b are the molar extinction coefficients of free HCQS and bound HCQS with RNA (RNA:HCQS), respectively at 330 nm. L_T = total concentration of HCQS (free + bound). The path length *(l)* of the cuvette is 1 cm and the unit of ε is in M^{-1} cm^{-1}, so the path length is not explicitly mentioned in the given equation (6) above. ε_f was calculated from the plot of absorbance against the concentration of HCQS and the obtained value of ε_f(330 nm) = 16960 M^{-1} cm^{-1} in 20 mM PB (Fig. S1A). Our Benesi-Hildebrand plot obtained from absorbance data (at 330 nm) is depicted in Fig. 1D. The intercept of this plot was found to be 12.36, and L_T is the total HCQS concentration (20 μM).

Using ε_f = 16960 M^{-1} cm^{-1} and L_T = 20 μM, from equation (6):

$$Intercept = \frac{1}{(\varepsilon_f - \varepsilon_b)L_T} \qquad (7)$$

which subsequently provides us with ε_b to be 12914.69 M^{-1} cm^{-1}.

Now considering the final absorbance of HCQS upon the addition of 500 μM RNA, (A_{total} = 0.29439 obtained from the last value of Fig. S1F corresponding to a [RNA] = 500 μM, and as marked in Fig. S1F) can be written as a combined absorbance of free drug and RNA-bound drug such as:

$$A_{total} = A_f + A_b \qquad (8)$$

$$A_{total} = \varepsilon_f L_f + \varepsilon_b L_b \; (assuming\ the\ path\ length = 1\ cm) \qquad (9)$$

Here, L_f is the free drug concentration and L_b is the bound drug concentration. The relation between L_T, L_f, and L_b is given by:

$$L_T = L_f + L_b \qquad (10)$$

From these above two equations (9 and 10), L_b was found to be 8.9 μM, corresponding to a bound fraction 8.9/20 = 0.44. Thus, both these independent approaches substantiate that 44% of the drug (HCQS) binds to RNA.

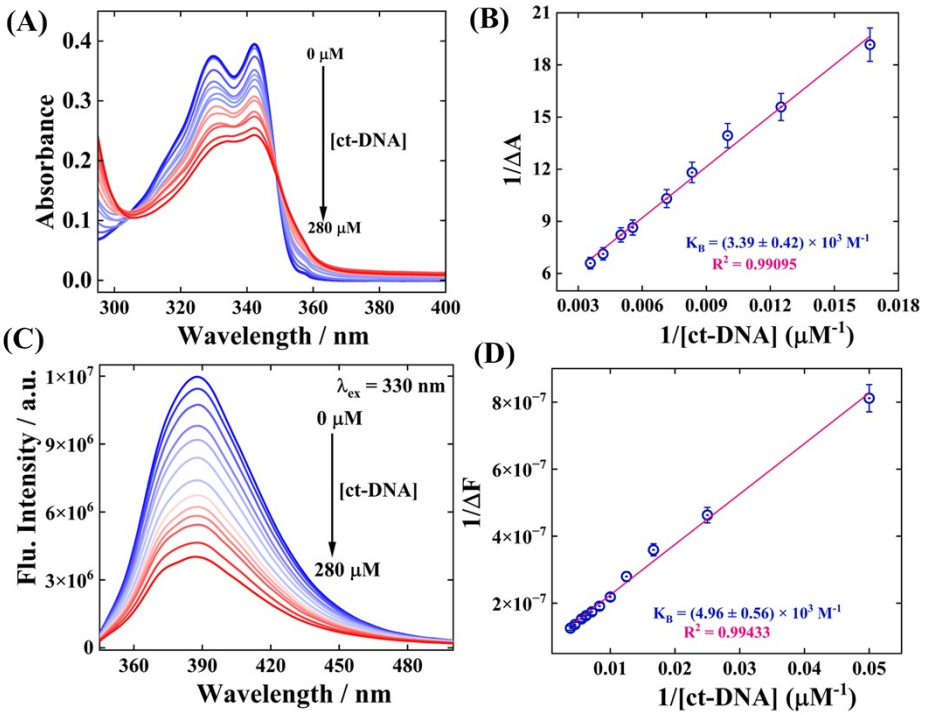

Fig. S2 Binding interactions of HCQS with calf thymus DNA (ct-DNA). (A) Absorption spectra of HCQS with increasing concentration of ct-DNA. (B) Benesi-Hildebrand plot of ct-DNA-HCQS interaction from absorption data. (C) Fluorescence spectra of HCQS with increasing concentration of ct-DNA, excited at 330 nm. (D) Benesi-Hildebrand plot of ct-DNA-HCQS interaction from fluorescence data. All experiments were carried out at pH ~7.4 and 298 K.

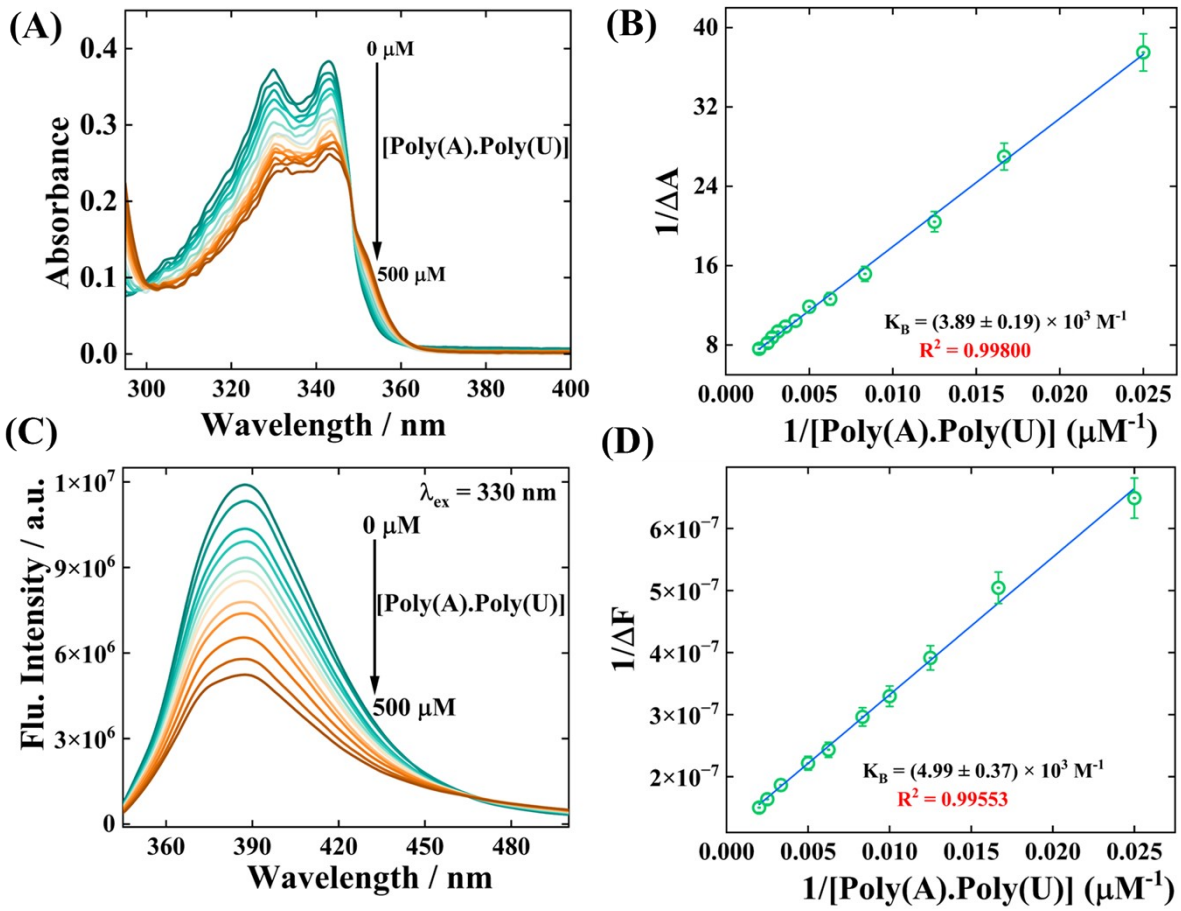

Fig. S3 Binding interactions of HCQS with polyadenylic acid-polyuridylic acid sodium salt (Poly(A).Poly(U)). (A) Absorption spectra of HCQS with increasing concentration of Poly(A).Poly(U). (B) Benesi-Hildebrand plot of Poly(A).Poly(U)-HCQS interaction from absorption data. (C) Fluorescence spectra of HCQS with increasing concentration of Poly(A).Poly(U), excited at 330 nm. (D) Benesi-Hildebrand plot of Poly(A).Poly(U)-HCQS interaction from fluorescence data. All experiments were carried out at pH ~7.4 and 298 K.

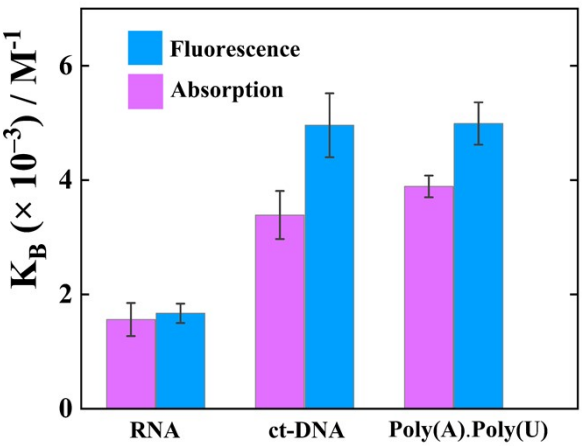

Fig. S4 Comparison plot of the binding constants of the interactions of HCQS with RNA, ct-DNA, and Poly(A).Poly(U) as obtained from absorption and fluorescence measurements.

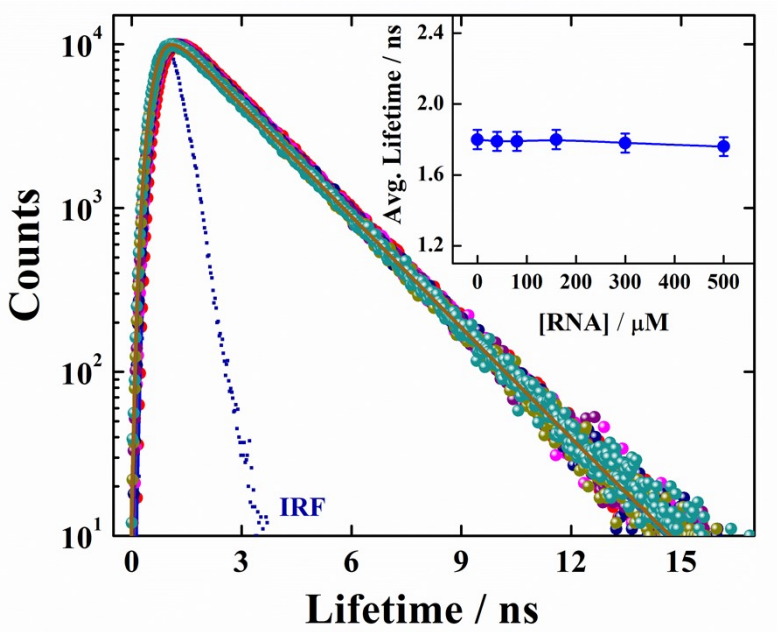

Fig. S5 Fluorescence lifetime decay profiles of HCQS with increasing concentrations of RNA. The inset represents the variations in the average fluorescence lifetime of HCQS with the incremental addition of RNA. The samples were excited at 340 nm, and lifetimes were collected at 388 nm. The concentration of HCQS was 20 μM.

Table S2. Fluorescence lifetime parameters of HCQS as a function of increasing concentration of RNA.

S. N.	System	α_1	τ_1 (ns)	α_2	τ_2 (ns)	$<\tau>^{\varphi}$ (ns)	χ^2
1.	20 μM HCQS + 0 μM RNA	0.05	0.17	0.95	1.89	**1.80**	1.03
2.	20 μM HCQS + 40 μM RNA	0.06	0.13	0.94	1.90	**1.79**	1.10
3.	20 μM HCQS + 80 μM RNA	0.06	0.10	0.94	1.90	**1.79**	1.02
4.	20 μM HCQS + 160 μM RNA	0.06	0.15	0.94	1.90	**1.80**	1.07
5.	20 μM HCQS + 300 μM RNA	0.07	0.12	0.93	1.90	**1.78**	1.00
6.	20 μM HCQS + 500 μM RNA	0.09	0.11	0.91	1.92	**1.76**	1.06

$\varphi = \pm 3\%$

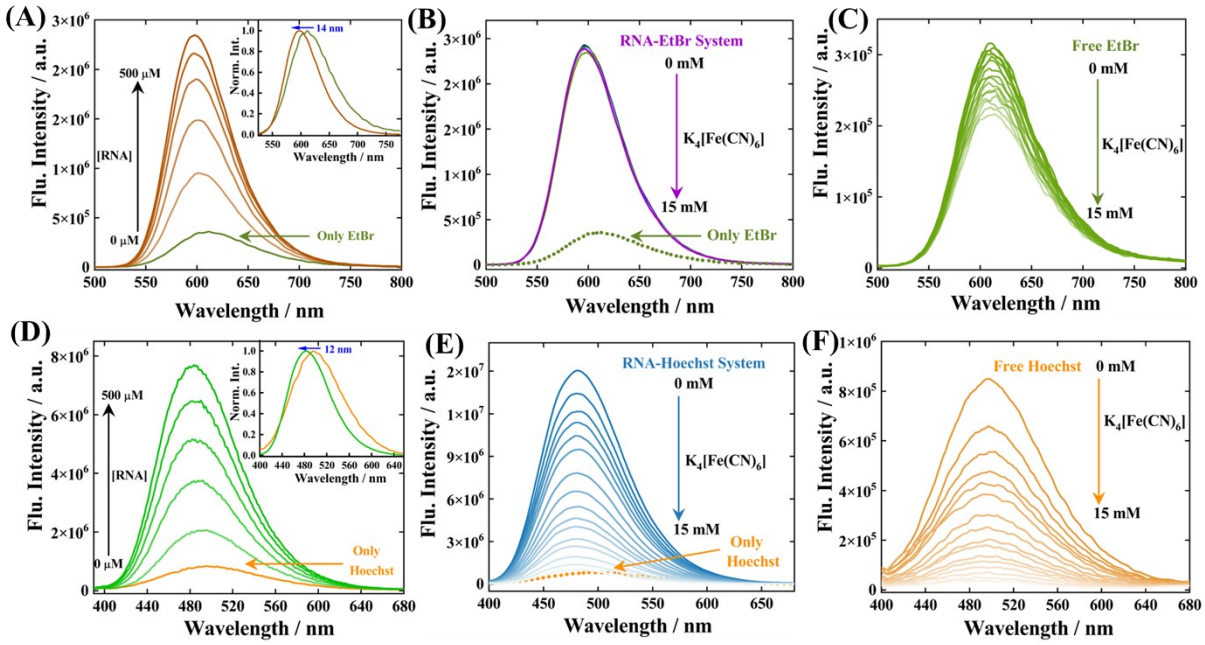

Fig. S6 (A) and (D) Binding of RNA with EtBr and Hoechst, respectively (insets of both represent blue shift observed in the emission maxima of dyes upon binding with RNA). $K_4[Fe(CN)_6]$-induced quenching of (B) RNA-EtBr system. (C) Free EtBr. (E) RNA-Hoechst system. (F) Free Hoechst.

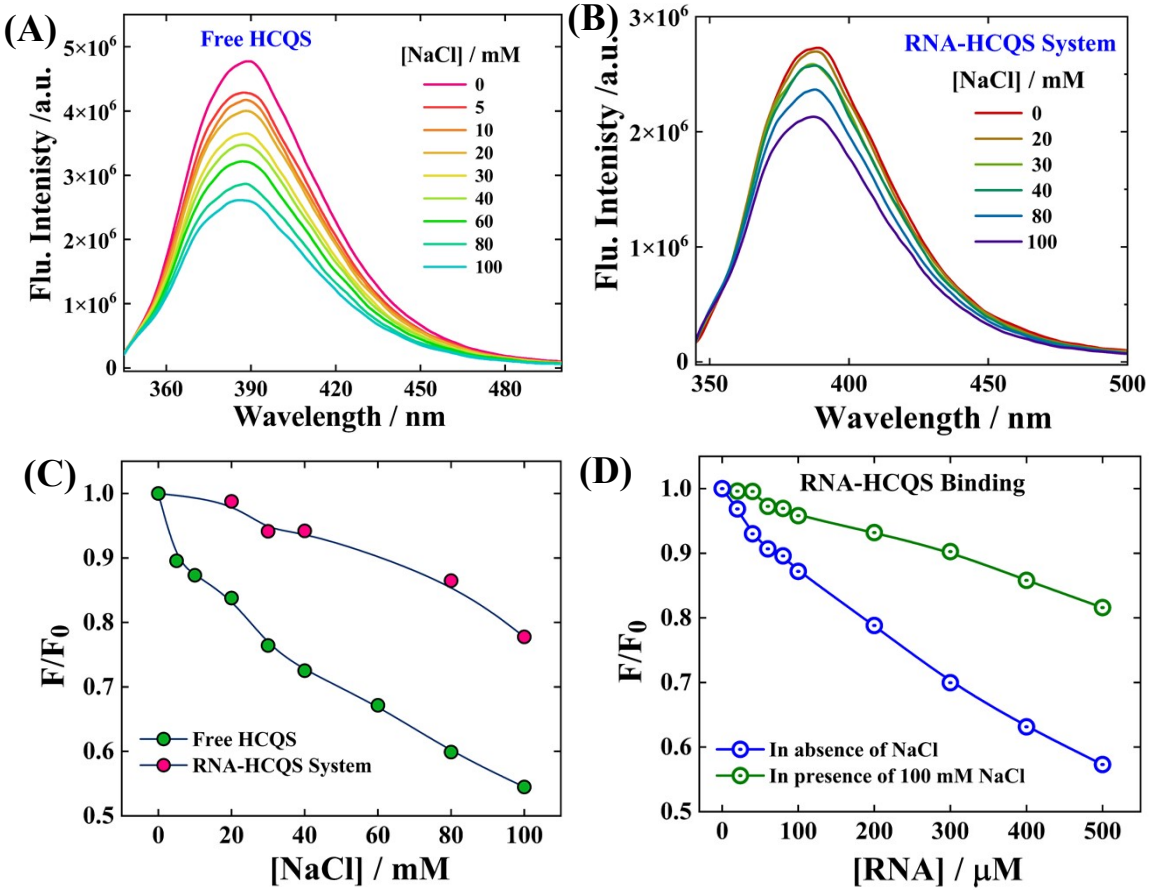

Fig. S7 Fluorescence quenching of (A) Free HCQS and (B) RNA-HCQS system in the presence of varying concentrations of NaCl. (C) Relative change in the fluorescence intensity of free HCQS and RNA-bound HCQS in the presence of NaCl. (D) Relative change in the fluorescence intensity of RNA-bound HCQS in the absence and presence of 100 mM NaCl.

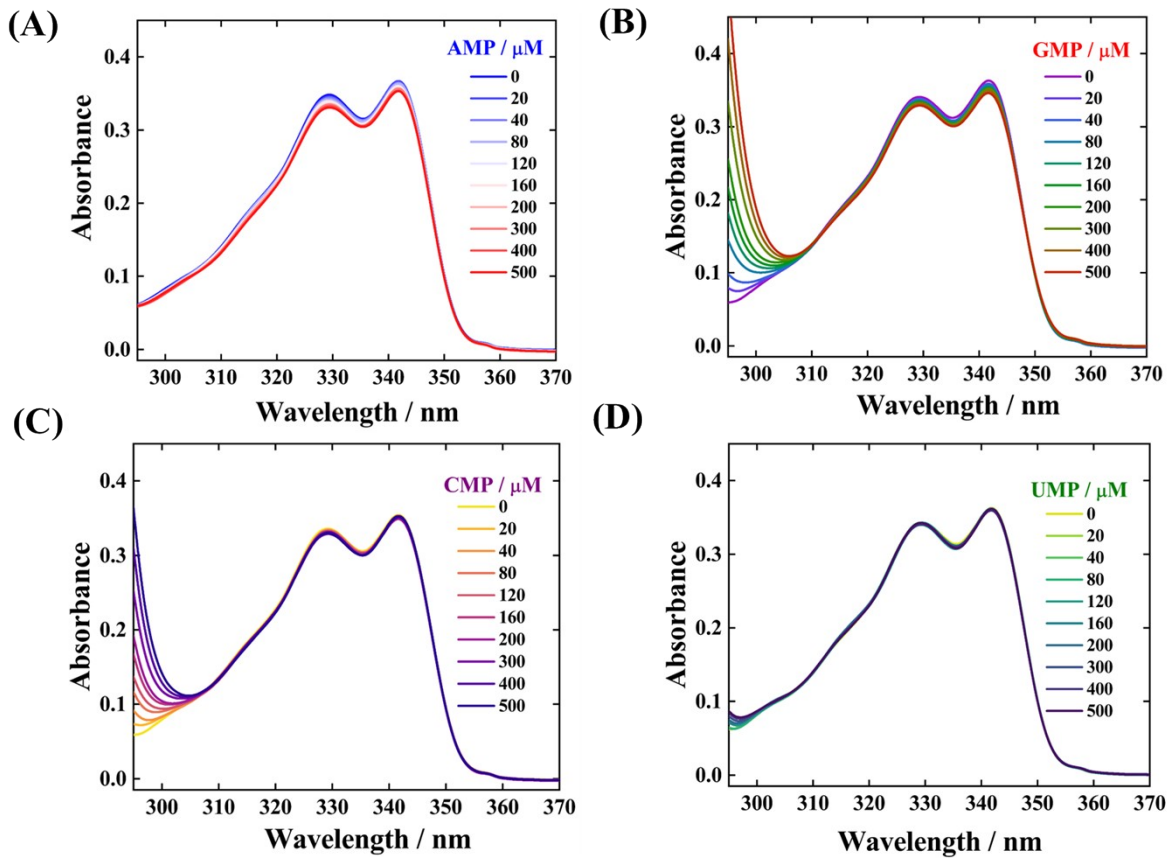

Fig. S8 Absorption spectra of HCQS with added (A) AMP, (B) GMP, (C) CMP, and (D) UMP nucleobases.

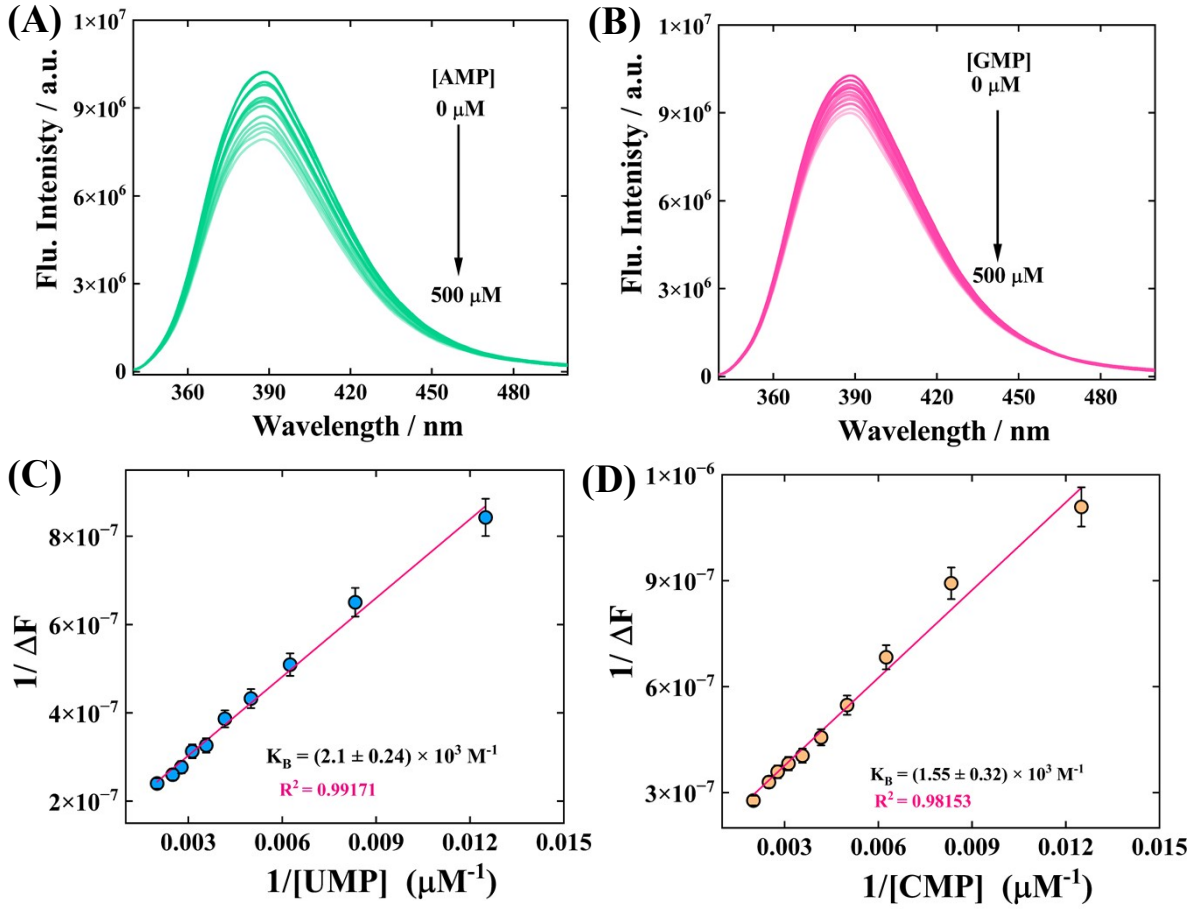

Fig. S9 Fluorescence quenching of HCQS with added (A) AMP nucleobase and (B) GMP nucleobase. Benesi-Hildebrand analysis of fluorescence data of (C) UMP and (D) CMP.

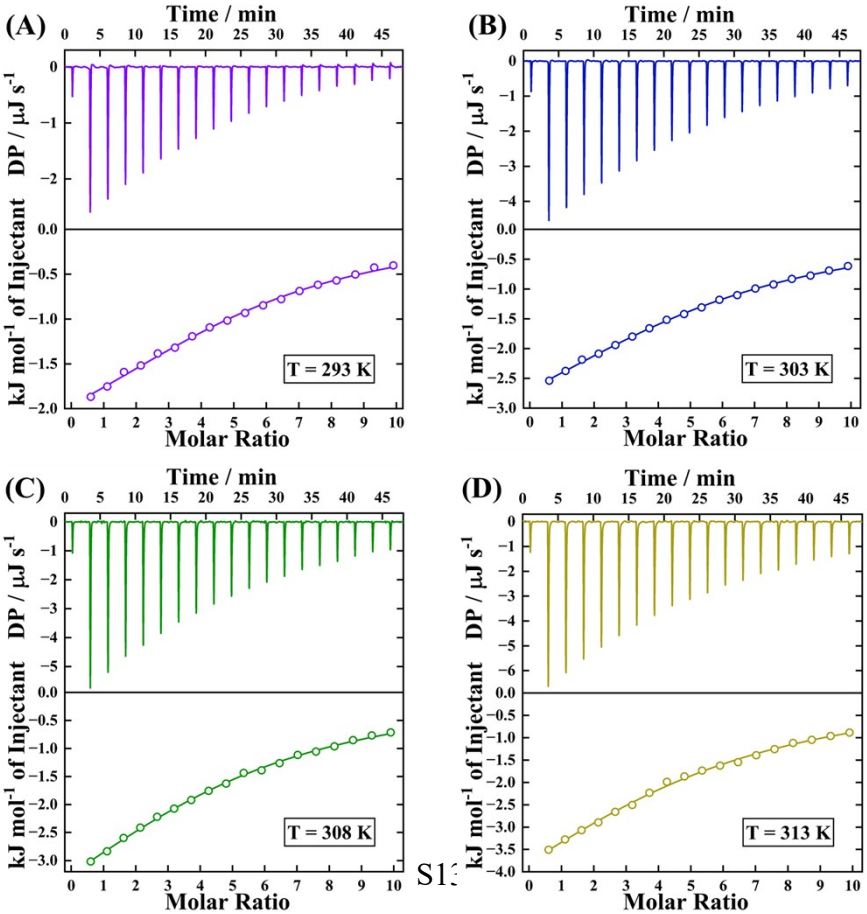

Fig. S10 ITC heat burst spikes of the addition of RNA to HCQS at different temperatures as marked in the figures.

Table S3 Thermodynamic parameters obtained from ITC experiments for RNA-HCQS interaction at different temperatures and for nucleobase (UMP, CMP)-HCQS interaction at 298 K.

Temperature (K)	K_a (M^{-1})	ΔH (kJ mol^{-1})	$T\Delta S$ (kJ mol^{-1})	ΔG (kJ mol^{-1})
293	$(1.703 \pm 0.15) \times 10^3$	-2.99 ± 0.14	15.15	−18.16
298	$(1.529 \pm 0.07) \times 10^3$	-3.57 ± 0.09	14.60	−18.2
303	$(1.345 \pm 0.08) \times 10^3$	-4.44 ± 0.16	13.72	−18.16
308	$(1.209 \pm 0.09) \times 10^3$	-5.90 ± 0.37	12.31	−18.2
313	$(1.145 \pm 0.12) \times 10^3$	-6.99 ± 0.56	11.34	−18.36
298 for UMP	$(1.043 \pm 0.09) \times 10^3$	-9.92 ± 0.87	7.32	−17.24
298 for CMP	$(1.145 \pm 0.12) \times 10^3$	-6.40 ± 0.48	11.42	−17.87

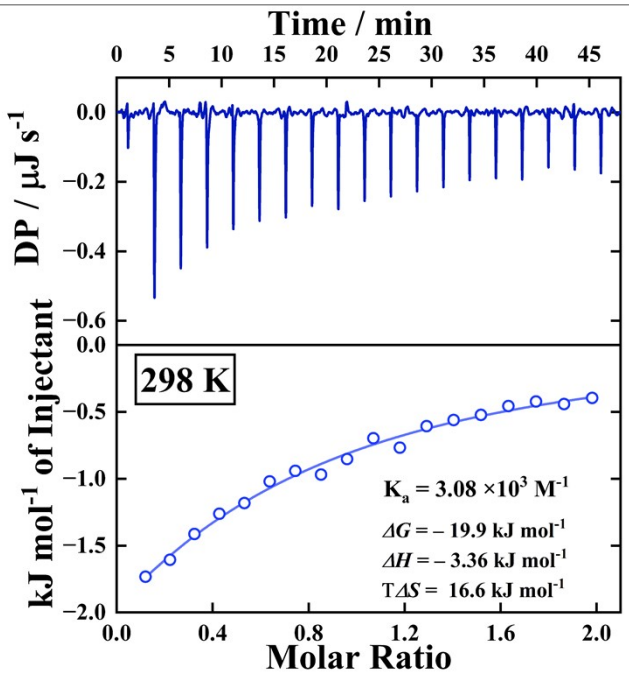

Fig. S11 ITC heat burst spikes of the addition of HCQS to RNA solution at 298 K, in 20 mM PB. [RNA] was kept at 100 μM in the cell and [HCQS] was kept at 1000 μM in the syringe. The dissociation constant ($K_d = 1/K_a$) has been estimated to be 324 μM.

To carry out a reverse titration, the HCQS (ligand) solution was titrated to RNA (macromolecule) solution. [HCQS] was kept at 1000 μM in the syringe and [RNA] was kept at 100 μM in the cell, the experiment was performed at 298 K in 20 mM PB, and the heat of dilution corresponding was determined by titrating free HCQS to buffer under identical conditions. The obaitned thermodynamic paramters are enlisted in Table S4.

The binding isotherm of HCQS to RNA can be depicted by the following relation:

$$[RNA] + [HCQS] \rightleftharpoons [RNA{:}HCQS]$$

Association constant $K_a = \frac{[RNA{:}HCQS]}{[RNA][HCQS]}$ and dissociation constant was determined by $K_d = 1/K_a$.

The fractional saturation was determined by the following equation:

$$Y = \frac{[L]}{[L] + K_d} \tag{11}$$

Here, *[L]* is the concentration of ligand, K_d is the dissociation constant and *Y* is the fractional saturation.

Table S4 Thermodynamic parameters obtained from ITC experiments for RNA-HCQS by two different approaches (i) RNA added to HCQS, (ii) HCQS added to RNA at 298 K.

Approach	K_a	K_d	ΔH (kJ mol^{-1})	$T\Delta S$ (kJ mol^{-1})	ΔG (kJ mol^{-1})
Approach 1 RNA in HCQS [RNA] = 10000 μM in syringe [HCQS] = 200 μM in cell	1.529×10^3 M^{-1}	654 μM	–3.57	14.6	–18.2

Approach 2 HCQS in RNA [HCQS] = 1000 μM in syringe [RNA] = 100 μM in cell	3.08×10^3 M^{-1}	324 μM	–3.36	16.6	–19.9

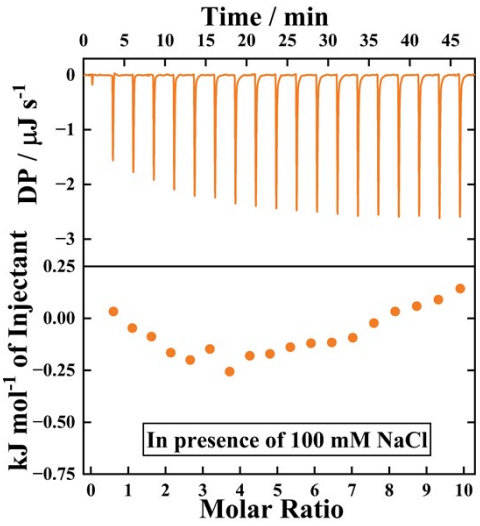

Fig. S12 ITC heat burst spikes for RNA-HCQS interaction in the presence of 100 mM NaCl.

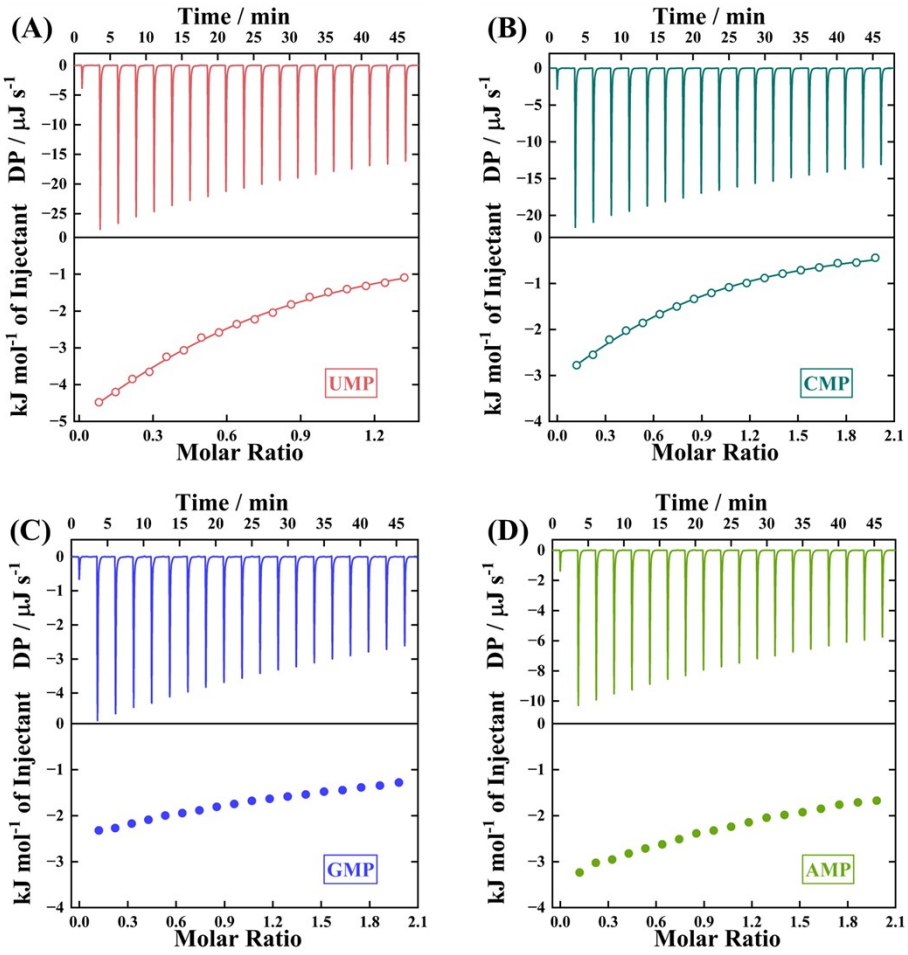

Fig. S13 ITC heat burst spikes of addition of different nucleobases to HCQS at 298 K. (A) UMP, (B) CMP, (C) GMP, and (D) AMP.

Table S5 Thermodynamic and binding parameters obtained from ITC and fluorescence spectroscopy for host-guest complexation of SCX4 with free HCQS and RNA-bound HCQS.

From Isothermal Titration Calorimetry				
System	**K_a (M^{-1})**	**ΔH (kJ mol^{-1})**	***TΔS (kJ mol^{-1})***	***ΔG (kJ mol^{-1})***
Free HCQS	$(3.26 \pm 0.17) \times 10^5$	–33.93 ± 0.22	-2.46	–31.46
RNA-Bound HCQS	$(0.94 \pm 0.05) \times 10^5$	–19.75 ± 0.23	8.66	–28.41
From Fluorescence Spectroscopy				
Free HCQS	$(8.4 \pm 0.9) \times 10^5$			
RNA-Bound HCQS	$(6.9 \pm 1.5) \times 10^5$			

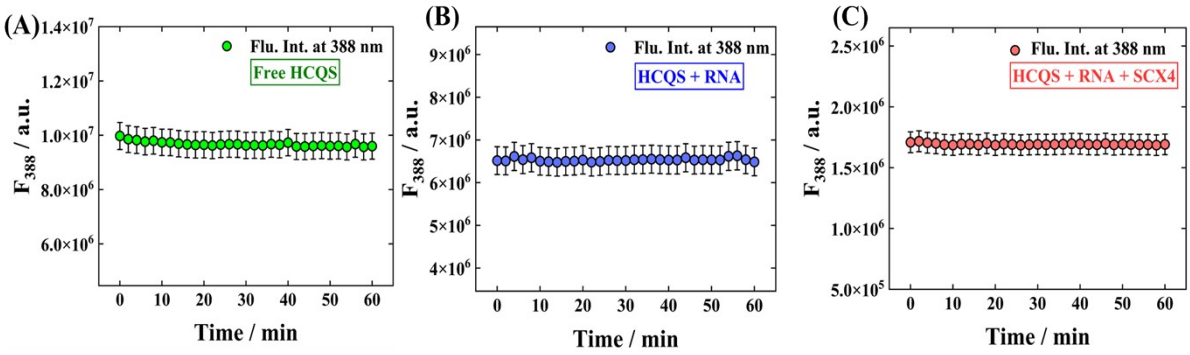

Fig. S14 Time-dependent emission spectra of free HCQS, RNA-bound HCQS, and RNA-bound HCQS after the addition of SCX4. All samples were excited at 330 nm and the emission was recorded at 388 nm as a function of time for 1 hr with the interval of 2 minutes. All experiments were performed at 298 K and in 20 mM PB (pH ~7.4).

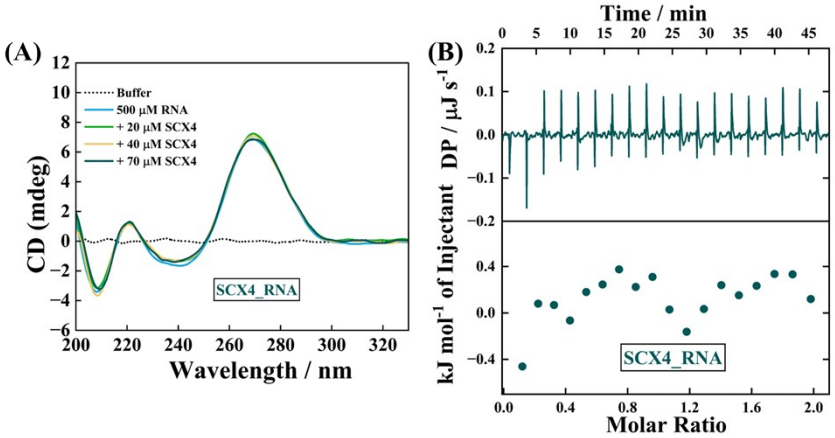

Fig. S15 (A) CD and (B) ITC profiles of addition of SCX4 to RNA in aqueous/buffer medium.

S1. J. L. Childs, M. D. Disney and D. H. Turner, *Proc. Natl. Acad. Sci. U.S.A* 2002, **99,** 11091–11096.

S2. A. X. Mendes, L. Caballero Aguilar, A. T. Do Nascimento, S. Duchi, M. Charnley, D. R. Nisbet, A. F. Quigley, R. M. I. Kapsa, S. Silva and S. E. Moulton, *ACS Appl. Bio Mater* 2024, **7,** 4175–4192.

S3. P. Mahato, S. Shekhar, S. Agrawal, S. Pramanik, and S. Mukherjee. *ACS Appl. Nano Mater.*, 2022, **5**, 7571–7579.

S4. A. Funke, and K. Weisz, *J. Phys. Chem. B* 2017, **121,** 5735–5743.

S5. S. Promtang, T. Sanguanphun, P. Chalorak, L. S. Pe, N. Niamnont, P. Sobhon and K. Meemon, *ACS Chem. Neurosci.* 2024, **15,** 2182–2197.

S6. S. Quraishi, D. Saha, K. Kumari, A. N. Jha and A. S. Roy, *Int. J. Biol. Macromol.* 2024, **257,** 128568–128583.

S7. A. S. Roy, D. R. Tripathy, S. Samanta, S. K. Ghosh and S. Dasgupta, *Mol. Biosyst.,* 2016, **12**, 1687–1701.